

DESY 97-040
 ITB-SB-97-18
 hep-ph/9703349
 March 1997

Two-loop matching of the dipole operators for $b \rightarrow s$ and $b \rightarrow sg$ ¹

Christoph Greub

Deutsches Elektronen-Synchrotron DESY,
 22603 Hamburg, Germany

Tobias Hurth

Institute of Theoretical Physics, SUNY at Stony Brook,
 Stony Brook, New York 11794-3840, USA

Abstract

The order α_s corrections to the Wilson coefficients of the dipole operators ($O_7; O_8$) at the matching scale $\mu = m_W$ are a crucial ingredient for a complete next-to-leading logarithmic calculation of the branching ratio for $b \rightarrow s$. Given the phenomenological relevance and the fact that this two-loop calculation has been done so far only by one group [1], we present a detailed re-calculation using a different method. Our results are in complete agreement with those in ref. [1].

¹Work supported in part by Schweizerischer Nationalfonds

1 Introduction

By definition, rare B meson decays only arise at the one loop level in the standard model (SM). Therefore these decays are particularly sensitive to effects from new physics. Among these decays, the inclusive modes like $B \rightarrow X_s$ are particularly interesting, because no specific model is needed to describe the final hadronic state in contrast to the exclusive decay modes. Indeed, heavy quark effective theory tells us that the decay width $\Gamma(B \rightarrow X_s)$ is well approximated by the partonic decay rate $\Gamma(b \rightarrow X_s)$ which can be analyzed in renormalization group improved perturbation theory. The class of non-perturbative effects which scales like $1/m_b^2$ is expected to be well below 10% [2]. This numerical statement is supposed to hold also for the recently discovered non-perturbative contributions which scale like $1/m_c^2$ [3].

Up to recently, only the leading logarithmic (LL) perturbative QCD corrections were calculated systematically [4]. The error of these calculations is dominated by a large renormalization scale dependence at the 25% level. The measured branching ratio $BR(B \rightarrow X_s) = (2.32 \pm 0.67) \cdot 10^{-4}$ reported in 1995 by the CLEO collaboration [5] overlaps with the estimates based on leading logarithmic calculations (or with some next-to-leading effects partially included) and the experimental and theoretical errors are comparable [6, 7, 8, 9, 10, 11]. However, in view of the expected increase in the experimental precision in the near future, it became clear that a systematic inclusion of the next-to-leading logarithmic (NLL) corrections becomes necessary [8]. This ambitious NLL enterprise was recently completed; combining the results of different groups [1, 6, 10, 12, 13, 14], the first complete theoretical prediction to NLL precision for the $b \rightarrow X_s + \gamma$ branching ratio was presented in [14]: $BR(B \rightarrow X_s) = (3.28 \pm 0.33) \cdot 10^{-4}$. This prediction is still in agreement with the CLEO measurement at the 2%-level. The theoretical error is twice smaller than in the leading logarithmic prediction. So the inclusive $B \rightarrow X_s + \gamma$ mode will provide an interesting test of the SM and its extensions when also more precise experimental data will be available.

Before discussing in some more detail the principle steps leading to a next-to-leading result for $b \rightarrow X_s$, we briefly have to recall the formalism. We use the framework of an effective low-energy theory with five quarks, obtained by integrating out the top quark and the W-boson. The effective Hamiltonian relevant for $b \rightarrow s$ and $b \rightarrow sg$ reads

$$H_{\text{eff}}(b \rightarrow s) = -\frac{4G_F}{2} \sum_{i=1}^8 C_i(\mu) O_i(\mu); \quad (1.1)$$

where $O_i(\mu)$ are the relevant operators, $C_i(\mu)$ are the corresponding Wilson coefficients, which contain the complete top- and W-mass dependence, and $\mu = V_{tb}V_{ts}$ with V_{ij} being the CKM matrix elements². Neglecting operators with dimension > 6 which are suppressed by higher powers of $1/m_{W,t}$ -factors and using the equations of motion for the operators, one arrives at the following basis³ of dimension 6 operators [15]

$$\begin{aligned} O_1 &= (\bar{c}_L \gamma_\mu b_L)(\bar{s}_L \gamma_\mu c_L); \\ O_2 &= (\bar{c}_L \gamma_\mu b_L)(\bar{s}_L \gamma_\mu c_L); \\ O_3 &= (\bar{s}_L \gamma_\mu b_L)(\bar{u}_L \gamma_\mu u_L) + \dots + (\bar{b}_L \gamma_\mu b_L); \end{aligned}$$

²The CKM dependence globally factorizes, because we work in the approximation $\mu = 0$.

³In [14] another basis was used. We comment on this in the summary.

$$\begin{aligned}
O_4 &= (s_L \quad b_L) \begin{matrix} h \\ (u_L \quad u_L) \end{matrix} + \dots + b_L \quad b_L \begin{matrix} i \\ i \end{matrix}; \\
O_5 &= (s_L \quad b_L) \begin{matrix} h \\ (u_R \quad u_R) \end{matrix} + \dots + b_R \quad b_R \begin{matrix} i \\ i \end{matrix}; \\
O_6 &= (s_L \quad b_L) \begin{matrix} h \\ (u_R \quad u_R) \end{matrix} + \dots + b_R \quad b_R \begin{matrix} i \\ i \end{matrix}; \\
O_7 &= (e=16^{-2}) s \quad (m_b(\mu_R) + m_s(\mu_L)) b \quad F \quad ; \\
O_8 &= (g_s=16^{-2}) s \quad (m_b(\mu_R) + m_s(\mu_L)) (\quad^A=2) b \quad G^A \quad :
\end{aligned}
\tag{1.2}$$

In the dipole type operators O_7 and O_8 , e and F (g_s and G^A) denote the electromagnetic (strong) coupling constant and field strength tensor, respectively.

It is well-known that the QCD corrections enhance the $b \rightarrow s$ decay rate by more than a factor of two; these QCD effects can be attributed to logarithms of the form $\frac{n}{s}(m_b) \log^m(m_b/M)$, where $M = m_t$ or $M = m_W$ and $m \geq n$ (with $n = 0, 1, 2, \dots$). Working to NLL precision means, that one is resumming all the terms of the form $\frac{n}{s}(m_b) \ln^n(m_b/M)$, as well as $\frac{n}{s}(m_b) (\frac{n}{s}(m_b) \ln^n(m_b/M))$. This is achieved by performing the following 3 steps:

Step 1 One has to match the full standard model theory with the effective theory at the scale $\mu = \mu_t$, where μ_t denotes a scale of order m_W or m_t . At this scale, the matrix elements of the operators in the effective theory lead to the same logarithms as the full theory calculation. Consequently, the Wilson coefficients $C_i(\mu_t)$ only pick up small QCD corrections, which can be calculated in fixed order perturbation theory. In the NLL program, the matching has to be worked out at the $O(\alpha_s)$ level.

Step 2 Then one performs the evolution of these Wilson coefficients from $\mu = \mu_t$ down to $\mu = \mu_b$, where μ_b is of the order of m_b . As the matrix elements of the operators evaluated at the low scale μ_b are free of large logarithms, the latter are contained in resummed form in the Wilson coefficients. For a NLL calculation, this RGE step has to be performed using the anomalous dimension matrix up to order α_s^2 .

Step 3 The corrections to the matrix elements of the operators $\langle \mathcal{O}_i(\mu_b) \rangle$ at the scale $\mu = \mu_b$ have to be calculated to order α_s precision.

The most difficult part in Step 1 is the two-loop (or order α_s^2) matching of the dipole operators, which has been worked out by Adel and Yao [1] some time ago. Step 3 basically consists of Bremsstrahlung corrections and virtual corrections. The Bremsstrahlung corrections, together with some virtual corrections needed to cancel infrared singularities, have been worked out by Ali and Greub [6, 10]; later, this part was confirmed and extended by [12]. Recently, a complete analysis of the virtual corrections (up to the contributions of the 4 Fermi operators with very small coefficients) were presented by Greub, Hurth and Wyler [13]. The main result of the latter analysis consists in a drastic reduction of the renormalization scale uncertainty from about 25% to about 6%. Moreover, the central value was shifted outside the 1- σ bound of the CLEO measurement. However, at that time, the essential coefficient $C_7(\mu_b)$ was only known to leading-log precision. It was therefore unclear, how much the overall normalization will be changed, when using the NLL value for $C_7(\mu_b)$. Very recently, the order α_s^2 anomalous matrix (step 2) has been completely worked out by Chetyrkin, Misiak and Munz [14]. Using the matching result of Adel and Yao, these authors got the next-to-leading result for $C_7(\mu_b)$.

Numerically, the LL and the NLL value for $C_7(b)$ are rather similar; the NLL corrections to the Wilson coefficient $C_7(b)$ lead to a change of the $b \rightarrow X_s$ decay rate which does not exceed 6% [14]: The new contributions can be split into a part which is due to the order s corrections to the matching (Step 1) and into a part stemming from the improved anomalous dimension matrix (Step 2). While individually these two parts are not so small (in the NDR scheme, which was used in [14]), they almost cancel when combined as illustrated in [14]. This shows that all the different pieces are numerically equally important. However, strictly speaking the relative importance of different NLO-corrections at the scale $\mu = \mu_b$, namely the order s corrections to the matrix elements of the operators (Step 3) and the improved Wilson coefficients C_i (Step 1+2), is a renormalization-scheme dependent issue; so we stress that the discussion above was done within the naive dimensional regularization scheme (NDR).

Each of the three steps implies rather involved computations: The calculation of the matrix elements (Step 3) involves two-loop diagrams where the full charm mass dependence has to be taken into account. Also the matching calculation (Step 1) involves two-loop diagrams both in the full and in the effective theory. Finally, the extraction of some of the elements in the $O(s)$ anomalous dimension matrix involves three-loop diagrams. Given the fact, that it took a rather long time until the leading logarithmic calculations performed by different groups converged to a common answer, it is certainly desirable that all three steps mentioned above should be repeated by other independent groups, and, maybe using other methods.

Making a step into this direction, we present in this paper a re-calculation of the two-loop matching of the dipole operators O_7 and O_8 . We extracted the $O(s)$ contributions of the corresponding Wilson coefficients C_7 and C_8 by calculating the on-shell processes $b \rightarrow s$ and $b \rightarrow sg$ in both versions of the theory up to order s . We worked out the two-loop integrals by using the Heavy Mass Expansion method [16], which we describe in some detail in section 2.4.

The rest of the paper is organized as follows. In section 2 we make some preparations for the two-loop calculations. We first explain how to extract the order s corrections to the Wilson coefficients $C_7(\mu_t)$ and $C_8(\mu_t)$ in principle. Then, in various subsections we discuss and illustrate the technical methods used. Sections 3, 4 and 5 are devoted to the computation of $C_{71}(\mu_t)$: In section 3 we calculate QCD corrections to $b \rightarrow s$ in the full theory together with the corresponding counterterm contributions, while in section 4 the same is done in the effective theory. Comparing the results from section 3 and section 4, we extract $C_{71}(\mu_t)$ in section 5. Similarly, sections 6, 7 and 8 are devoted to the computation of $C_{81}(\mu_t)$: In section 6 we calculate QCD corrections to $b \rightarrow sg$ in the full theory together with the corresponding counterterm contributions, while in section 7 the same is done in the effective theory. Comparing the results from section 6 and section 7, we extract $C_{81}(\mu_t)$ in section 8. Finally, we give a brief summary in section 9.

2 Preparations for the two-loop calculations

2.1 Strategy for extracting C_{71} and C_{81}

Let \hat{M} denote the (on-shell) $b \rightarrow s$ matrix element calculated in the effective theory. \hat{M} can be written in the form

$$\hat{M} = \sum_i C_i(\mu) h_{i1}(\mu) ; \quad h_{i1}(\mu) = \langle s | \mathcal{O}_i(\mu) | b \rangle ; \quad (2.1)$$

To keep the notation simpler, we denote the matching scale by μ instead of μ_{WT} . Making use of the ϵ -expansion for $C_i(\epsilon)$ and $O_i(\epsilon)$

$$C_i(\epsilon) = C_{i0}(\epsilon) + \frac{\epsilon}{4} C_{i1}(\epsilon) + \dots; \quad hO_i(\epsilon) = hO_i(\epsilon)i_0 + \frac{\epsilon}{4} hO_i(\epsilon)i_1 + \dots; \quad (2.2)$$

we get the corresponding expansion for \hat{M} in the form

$$\hat{M} = C_{i0}(\epsilon) hO_i(\epsilon)i_0 + \frac{\epsilon}{4} (C_{i0}(\epsilon) hO_i(\epsilon)i_1 + C_{i1}(\epsilon) hO_i(\epsilon)i_0) + \dots; \quad (2.3)$$

On the other hand, let M denote the $b \rightarrow s$ matrix element evaluated in the full theory after discarding power suppressed terms of order $1/m_W^3$; M has the expansion

$$M = M_0 + \frac{\epsilon}{4} M_1 + \dots; \quad (2.4)$$

Requiring $M = \hat{M}$ and taking the coefficient of ϵ^1 , we get the $O(\epsilon)$ matching condition

$$M_1 = C_{i0}(\epsilon) hO_i(\epsilon)i_1 + C_{i1}(\epsilon) hO_i(\epsilon)i_0; \quad (2.5)$$

All coefficients in eq. (2.5) are known [17, 18], except C_{71} and C_{81} . As C_{81} comes together with $h\mathcal{O}_8(\epsilon)i_0$, which is zero, eq. (2.5) has only one unknown, viz. C_{71} , i.e., just what we want to extract.

The discussion for the extraction of C_{81} goes exactly along the same lines, using the process $b \rightarrow sg$ instead of $b \rightarrow s$.

A general remark is in order here. One could also match on-shell Greens functions instead of on-shell matrix elements. However, in this case one is not allowed to work in the operator basis given in eq. (1.2), because one has used the equations of motion for the operators to get this 8 dimensional basis. This Hamiltonian therefore only reproduces on-shell matrix elements correctly [19]. As we would have to work in the on-shell basis when matching Greens functions, we preferred to do on-shell matching. There is of course a price to pay: The on-shell processes $b \rightarrow s$ and $b \rightarrow sg$ are plagued with infrared singularities, which have to be treated carefully. However, as we will see later, this is not a real problem.

2.2 Technical details

We work in $d = 4 - 2\epsilon$ dimensions; in the full theory we use anticommuting ϵ , which should not be a problem, because there are no closed fermion loops involved. We also use this naive dimensional regularization scheme (NDR) in the effective theory. The calculations are done in the 't Hooft-Feynman gauge (electroweak sector) and the gluon propagator is taken in the Feynman gauge. To avoid Euler Γ_E terms and $\ln(4)$ factors in our expressions, we introduce the renormalization scale in the form $\mu^2 \exp(\epsilon) = (4\pi)^{\epsilon} \overline{MS}$ subtraction then corresponds to subtracting the poles in ϵ . Besides the ultraviolet singularities also the infrared singularities are dimensionally regularized. As we could clearly separate infrared and ultraviolet singularities, we labeled the infrared poles by the index ir (e.g., $1/\epsilon_{ir}$). We put $m_s = 0$, except in situations where mass singularities appear, i.e., we treat m_s as a regulator of these singularities. We work in the approximation $\alpha_s = 0$. To keep the formulae more compact, we put immediately $Q_u = 2/3$ ($Q_d = -1/3$) for up-type (down-type) quark charges. For the same reason we also immediately insert the numerical values for the color factors in the $b \rightarrow sg$ case.

⁴Of course C_{71} and C_{81} are also known from Adelman and Yao [1], but this is what we want to check.

2.3 Reducing the number of diagrams

For reasons of gauge invariance, we know that the final result for the $b \rightarrow s$ matrix element can be written in the form

$$M(b \rightarrow s) = F(\text{masses, couplings}) \cdot \text{hs } \mathcal{D}_7 \mathcal{P}_{\text{tree}} : \quad (2.6)$$

For $m_s = 0$, the quantity $\text{hs } \mathcal{D}_7 \mathcal{P}_{\text{tree}}$ is given by

$$\frac{16}{e} \text{hs } \mathcal{D}_7 \mathcal{P}_{\text{tree}} = 2m_b u(p^0) \not{q} R u(p) = u(p^0) \not{2m_b^2 - L - 4m_b(p'')R} u(p) ; \quad (2.7)$$

where $u(p^0)$ and $u(p)$ are the Dirac spinors for the s and the b quarks, respectively, and q'' the momentum (polarization vector) of the photon. In the last step we used $q = (p - p^0)$ and $q'' = 0$, where $p(p^0)$ is the momentum of the b - (s -) quark. When calculating a given Feynman diagram, it is sufficient to work out only the term proportional to $(p'')R$. After adding all the diagrams, the full answer can be reconstructed by means of eq. (2.7). This reduces the number of diagrams; e.g., when calculating the $O(1/s)$ corrections for $b \rightarrow s$ in the full theory, "only" the graphs in Fig. 2 have a non-zero projection on the term $(p'')R$.

A similar projection for the process $b \rightarrow sg$ (with obvious changes) can also be obtained.

2.4 Method for calculating of the two-loop diagrams

To extract C_{71} and C_{81} various one- and two-loop diagrams have to be calculated in both versions (full/effective) of the theory. As the one-loop diagrams are straightforwardly obtained by conventional techniques, we directly move to the two-loop diagrams. When working out $b \rightarrow s$ and $b \rightarrow sg$ in the effective theory at the matching scale m_W , the only two-loop contributions leading to terms of order $1/s$ are those associated with the operator O_2 . For the $b \rightarrow s$ case, these terms have been obtained in [13]. We anticipate, that in the corresponding full theory calculation a term appears which can be identified with the O_2 contribution in the effective theory. Consequently, the O_2 contribution is not needed explicitly for extracting C_{71} and C_{81} .

Therefore, we directly discuss the calculation of the two-loop contributions in the full theory. In order to match dimension 6 operators, it is sufficient to extract the terms of order m_b^2/M^2 ($M = m_W; m_t$) from the full-theory matrix elements for $b \rightarrow s$ and $b \rightarrow sg$ (terms suppressed by additional powers of m_b/M correspond to higher dimensional operators in the effective theory). A systematic expansion of the matrix elements in inverse powers of M can naturally be obtained by using the well-known Heavy Mass Expansion (HME). In our context we use this HME only as a method for working out the dimensionally regularized two-loop Feynman graphs (and not to get directly renormalized quantities). The theory of asymptotic expansions of Feynman diagrams is already a textbook matter [20]⁵. Therefore, we only recall those properties of the HME, which are of practical importance for our calculation (for the mathematical foundations

⁵The idea of deriving operator product expansions using subtractions of leading asymptotics goes back to Zimmermann [21]. Later this idea was systematically developed within the BPHZ scheme [22]. The simple explicit formulae for asymptotic expansion within dimensional regularisation like (2.8) have been systematically derived in [16].

of this method we refer to the literature [16]):

Suppose that all the masses of a given Feynman diagram can be divided into a set of large $\underline{M} = \{m_1, m_2, \dots\}$ and small $\underline{m} = \{m_1, m_2, \dots\}$ masses and assume that all external momenta $\underline{q} = \{q_1, q_2, \dots\}$ are small compared to the scale of the large masses \underline{M} ; then the statement is that the dimensionally regularised (unrenormalized) Feynman integral F associated with the Feynman diagram can be written as

$$F \stackrel{\underline{M} \rightarrow \infty}{\sim} \sum_{\gamma} T_{\underline{q}, \underline{m}} F(\underline{q}; \underline{m}; \underline{M}) \quad ; \quad (2.8)$$

where the sum is performed over all subgraphs of which fulfill the following two conditions simultaneously:

contains all lines with heavy masses (\underline{M}) and

consists of connectivity components that are one-particle-irreducible with respect to lines with small masses (\underline{m}).

Here some clarifying remarks are in order:

The operator T performs a Taylor expansion in the variables \underline{q} and \underline{m} , where \underline{m} denotes the set of light masses in and \underline{q} denotes the set of all external momenta with respect to the subgraph; to be more specific, an external momentum with respect to the subgraph can be an internal momentum with respect to the full graph. F_{γ} denotes the Feynman integral corresponding to the reduced graph $\gamma = \Gamma \setminus \gamma$. Note that the operator T is understood to act directly on the integrand of the subgraph. The decomposition of the original, say 1-loop-diagram into the subdiagram and the diagram γ is achieved in the corresponding Feynman integral by factorizing the product of scalar propagators as $\frac{1}{k^2 - m^2} = \frac{1}{k^2 - M^2} \sum_{n=0}^{\infty} \left(\frac{m^2}{k^2 - M^2} \right)^n$ such that

$$F = \sum_{\gamma} T_{\underline{q}, \underline{m}} F_{\gamma} = \sum_{\gamma} \int d^4k_1 \dots d^4k_{l_{\gamma}} \mathcal{I}_{\gamma}(\underline{q}; \underline{m}; \underline{M}) \quad ; \quad (2.9)$$

The full graph Γ is always a subgraph contributing in the sum \sum_{γ}^{Γ} .

It is instructive to look at the special case where all masses are large compared to the external momenta in a given diagram. In this case only the full graph contributes to the sum in (2.8). The complete HME expansion reduces to a naive Taylor expansion in the external momenta of the integrand of the Feynman integral:

$$F \stackrel{\underline{M} \rightarrow \infty}{\sim} T_{\underline{q}} F(\underline{q}; \underline{M}) \quad (2.10)$$

The Taylor operator T introduces additional spurious IR- or UV-divergences in the various terms of the sum \sum_{γ}^{Γ} , as we will see in an explicit example below. It is a nontrivial property of the HME that all these artificial divergences cancel after making a summation over all possible subgraphs. For our calculations this property provides a nontrivial check for the individual diagrams, as this cancellation has to happen diagram by diagram.

Now we illustrate this rather formal description for the diagram in Fig 1b, for an internal top quark and denote it D_{top} . It belongs to the Set1 in Fig 2. The W^- - and Z -exchange contributions

are understood to be added. The corresponding Feynman integral has the following form (the Dirac spinors $\bar{u}(p^0)$ and $u(p)$ are amputated):

$$D_{\text{top}} = X \exp(2\epsilon_E) (4)^2 \int \frac{d^d r}{(2)^d} \int \frac{d^d l}{(2)^d} \frac{D_{\text{irac}_{1t}}}{(p-q+r)^2 m_s^2 r^2} \frac{D_{\text{irac}_{2t}}}{[(l+r)^2 m_t^2 (l^2 - m_t^2) ((l+q)^2 - m_t^2)]} \frac{1}{(l+p-q)^2 m_W^2} \quad (2.11)$$

In (2.11) the functions $D_{\text{irac}_{1t}}$ and $D_{\text{irac}_{2t}}$ are the respective Dirac structures, whose explicit form is not important for explaining the principle steps of the expansion. The constant X collects all the remaining constant factors like coupling constants and CKM-factors.

We find two subdiagrams of D_{top} which fulfill the two conditions given below eq. (2.8): The first contribution of the HME corresponding to the subdiagram $_1$ shown in Fig. 1c is given by

$$D_{\text{top}}^1 = X \exp(2\epsilon_E) (4)^2 \int \frac{d^d r}{(2)^d} \int \frac{d^d l}{(2)^d} \frac{D_{\text{irac}_{1t}}}{(p-q+r)^2 m_s^2 r^2} T_{r p q} \frac{D_{\text{irac}_{2t}}}{[(l+r)^2 m_t^2 (l^2 - m_t^2) ((l+q)^2 - m_t^2)]} \frac{1}{(l+p-q)^2 m_W^2} \quad (2.12)$$

The second contribution is the naive one, $_2 = D_{\text{top}}$ (see Fig. 1d):

$$D_{\text{top}}^2 = X \exp(2\epsilon_E) (4)^2 \int \frac{d^d r}{(2)^d} \int \frac{d^d l}{(2)^d} T_{p q} \frac{D_{\text{irac}_{1t}}}{(p-q+r)^2 m_s^2 r^2} \frac{D_{\text{irac}_{2t}}}{[(l+r)^2 m_t^2 (l^2 - m_t^2) ((l+q)^2 - m_t^2)]} \frac{1}{(l+p-q)^2 m_W^2} \quad (2.13)$$

So we end up with

$$D_{\text{top}} \stackrel{M}{=} D_{\text{top}}^1 + D_{\text{top}}^2 \quad (2.14)$$

The integrals are considerably simplified after the Taylor operation T and can be solved analytically after introducing Feynman parametrization. We mention that the Dirac algebra has been done with the algebraic program REDUCE [23] and the integrals have been done with the symbolic program MAPLE [24].

As mentioned above we can discard terms of order $1/M^3$. Simple dimensional arguments tell us that we have to perform the Taylor operation T up to second order in the external momenta r, p, q in D_{top}^1 and also up to second order in p, q in D_{top}^2 . Restoring all the factors which we symbolized by X , and projecting on the term $(p'')R$, we get

$$D_{\text{top}} = \frac{4iG_F}{2} \frac{t}{4} C_F \frac{e}{16^2} (4m_b) (p'')R \left(d_{\text{top}}^1 + d_{\text{top}}^2 \right) \quad (2.15)$$

The quantities d_{top}^1 and d_{top}^2 are given by ($z = (m_t - m_W)^2$):

$$d_{\text{top}}^1 = \frac{S}{(1-2 \ln(m_b/m_W)) - 2 \ln(m_s/m_b) + 4 \ln(-m_W)} \frac{9z^2 - 8z + 2}{36(z-1)^4} \ln^2 z + \frac{11z^4 - 14z^3 + 234z^2 - 180z + 24}{108(z-1)^4} \ln z - \frac{229z^3 + 15z^2 + 744z - 538}{648(z-1)^3} \quad (2.16)$$

$$\begin{aligned}
d_{\text{top}}^2 = & + \frac{S}{\text{ir}} (1 + 4 \ln(-m_W)) + \frac{108z \ln z + 60z^4}{108(z-1)^4} \frac{258z^3 + 468z^2}{m_W^4} \frac{294z + 24}{m_W^4} \\
& + \frac{9z^2 + 10z + 2}{12(z-1)^4} \ln^2 z + \frac{142z^4}{108(z-1)^4} \frac{538z^3 + 753z^2}{108(z-1)^4} \ln z \\
& + \frac{z^4}{18(z-1)^4} \frac{40z^3 + 27z^2}{18(z-1)^4} \frac{10z}{2} \text{Li}\left(1 - \frac{1}{z}\right) + \frac{67z^3 + 2343z^2}{648(z-1)^3} \frac{2766z + 230}{648(z-1)^3} ; \quad (2.17)
\end{aligned}$$

where the function S is

$$S = \frac{(54z^2 + 48z - 12) \ln z + 11z^4}{108(z-1)^4} \frac{14z^3 + 27z^2}{108(z-1)^4} \frac{38z + 14}{108(z-1)^4} ; \quad (2.18)$$

The $1=$ poles in d_{top}^1 correspond to spurious ultraviolet singularities produced in the r -integration after expanding the subdiagram γ_1 . The $1=_{\text{ir}}$ poles in d_{top}^2 on the other hand arise due to the worsened infrared behaviour induced when expanding the s -quark propagator. As we explicitly see, these artificial singularities cancel when adding d_{top}^1 and d_{top}^2 .

We now discuss the corresponding diagram D_{charm} where the internal top quark is replaced by the (light) charm quark. The quantities D_{charm}^1 and D_{charm}^2 corresponding to the subdiagrams γ_1 and γ_2 (see Fig. 1c,d) are given by the analogous formulae (2.12) and (2.13), where m_t is replaced by m_c and the Taylor operator $T_{r,p,q}$ in (2.12) is replaced by T_{r,p,q,m_c} and $T_{p,q}$ in (2.13) by T_{p,q,m_c} . As we are discarding terms of order $1=M^3$, it turns out that only the zeroth order term in the m_c expansion has to be retained; this amounts to putting $m_c = 0$ in D_{charm}^1 and D_{charm}^2 .

Moreover, in the charm-case there is a third contribution to the HME which corresponds to the subdiagram γ_3 in Fig. 1e. The latter consists of the W^- -line only. As we neglect terms of order $1=M^3$, the Taylor expansion of the corresponding Feynman integral just amounts to replace the W and γ propagator by $i=m_W^2$ and $i=m_W^2$, respectively. As the Feynman integral of the γ diagram has an additional factor of order $(m_c m_b)=m_W^2$ from the Yukawa couplings, only the fourFermi version of the W exchange diagram effectively contributes to D_{charm}^3 . Stated differently, D_{charm}^3 is directly related to the O_2 contribution in the effective theory. Of course, this is not surprising when keeping in mind how the effective Hamiltonian is constructed.

To summarize, D_{charm} is given by

$$D_{\text{charm}} \stackrel{M^3}{=} D_{\text{charm}}^1 + D_{\text{charm}}^2 + D_{\text{charm}}^3 ; \quad (2.19)$$

2.5 The matching to leading-log precision

To establish some lowest order matching functions which are frequently used in the following sections and in order to explain an important subtlety in the NLL matching calculation, we recall the results of the LL matching: In the full theory the lowest order matrix elements M_0 for $b \rightarrow s$ and $b \rightarrow sg$ are obtained by expanding the diagrams shown in Fig. 1a up to second order in the external momenta. The results read in $d = 4 - 2\epsilon$ dimensions

$$M_0(b \rightarrow s) = \frac{4iG_F}{2} t K_{70} \text{hs} \langle \bar{\psi} \gamma_7 \psi \rangle ; \quad M_0(b \rightarrow sg) = \frac{4iG_F}{2} t K_{80} \text{hsg} \langle \bar{\psi} \gamma_8 \psi \rangle ; \quad (2.20)$$

where the functions K_{70} and K_{80} have an expansion in ϵ of the form

$$K_{70} = K_{700} + \epsilon K_{701} + \epsilon^2 K_{702} + \dots ; \quad K_{80} = K_{800} + \epsilon K_{801} + \epsilon^2 K_{802} + \dots : \quad (2.21)$$

On the other hand, the lowest order result \hat{M}_0 in the effective theory reads (also in $d = 4 - 2\epsilon$ dimensions)

$$\hat{M}_0(b!s) = C_{70} \text{hs } \mathcal{P}_7 \text{ji} ; \quad \hat{M}_0(b!sg) = C_{80} \text{hsg } \mathcal{P}_8 \text{ji} : \quad (2.22)$$

As the matching is understood to be done in 4 dimensions, we get the connections

$$C_{70} = K_{700} ; \quad C_{80} = K_{800} : \quad (2.23)$$

Therefore, in d dimensions M_0 and \hat{M}_0 differ by terms of order ϵ . This detail becomes an important subtlety when going to higher loop orders; we best explain this by means of an example: one type of order ϵ corrections is given by multiplying the lowest order result by ultraviolet singular \overline{Z}_2 factors which are the same for both versions of the theory. In the full theory, this leads to finite terms proportional to K_{701} (and K_{801}); the corresponding terms in the effective theory are not generated.

When working out the two-loop integrals corresponding to the diagrams in Figs. 2 and 3 in the full theory for $b!s$ (or $b!sg$), there are contributions in which the dimensionally regularized lowest order result, taken up to first or second order in ϵ , factorizes. As we will see later, the infrared singularity structure is precisely of this form. As we will use the explicit expressions for the Inami-Lin [25] functions K_{700} , K_{800} , K_{701} and K_{801} at several places, we list them here. Using $z = (m_t/m_W)^2$, they read

$$K_{700} = C_{70} = \frac{z [6z(3z-2) \ln z - (z-1)(8z^2+5z-7)]}{24(z-1)^4} \quad (2.24)$$

$$K_{800} = C_{80} = \frac{z [6z \ln z + (z-1)(z^2-5z-2)]}{8(z-1)^4} \quad (2.25)$$

$$K_{701} = \frac{z^h \frac{18z(3z-2) \ln^2 z + (44z^3 - 314z^2 + 324z - 96) \ln z + 56z^3 - 35z^2 - 56z + 35}{144(z-1)^4} + 2K_{700} \ln(-m_W)}{\quad} \quad (2.26)$$

$$K_{801} = \frac{z^h \frac{18z \ln^2 z + (10z^3 - 28z^2 + 108z - 48) \ln z + 25z^3 - 118z^2 + 119z - 26}{48(z-1)^4} + 2K_{800} \ln(-m_W)}{\quad} \quad (2.27)$$

3 $b!s$ in the full theory

In section 3.1 we present the results for the dimensionally regularized matrix element M for $b!s$ in the full theory. In section 3.2 we discuss the various counterterm contributions.

3.1 Two-loop Feynman diagrams

As in eq. (2.4), we write the $b \rightarrow s$ matrix element M in the form $M = M_0 + \frac{s}{4} M_1$. When using the "reduction technique" described in section 2.3, the complete list of two-loop diagrams contributing to M_1 is given in Fig. 2, where the cross stands for the possible locations where the photon can be emitted. Note that diagram 5b in Fig. 2 does not contribute in the limit $m_s = 0$. We write the result for M_1 in the form

$$\frac{s}{4} M_1 = V \left(R_t^{1+2} + R_c^{1+2} + R_c^3 \right); \quad (3.1)$$

where V is an abbreviation for the often occurring quantity

$$V = \frac{4iG_F}{\sqrt{2}} \frac{t}{4} C_F \text{hs } \mathcal{D}_7 \text{bi}_{\text{tree}}; \quad C_F = \frac{4}{3}; \quad (3.2)$$

In eq. (3.1) R_t^{1+2} (R_c^{1+2}) denotes the sum of the first and second contribution in the Heavy Mass Expansion (HME) (see section 2.4) of the dimensionally regularized (unrenormalized) Feynman integrals for internal top (charm) quark; R_c^3 is the third contribution in the HME, which has to be considered only for the light internal quarks, which in our present case is the charm quark ($m_u = 0$). According to the HME, R_c^3 is obtained by working out the charm loops using the four-Fermi approximation of the W -propagator. Stated differently, R_c^3 is directly related to the order s contribution of matrix element of the operator O_2 , provided the latter is evaluated in the NDR scheme; more precisely,

$$R_c^3 = \hat{R}_2 \quad (3.3)$$

where \hat{R}_2 is the quantity defined through the equation

$$\text{hs } \mathcal{D}_2 \text{bi} = \frac{s}{4} C_F \text{hs } \mathcal{D}_7 \text{bi}_{\text{tree}} \hat{R}_2; \quad (3.4)$$

As the same contribution is also present in the effective theory, we will not need to know R_c^3 explicitly⁶ in order to extract the order s corrections in the Wilson coefficient $C_{71}(m_W, t)$. Making use of the various K -functions given in (2.24)–(2.27) and denoting $r = (m_s = m_b)^2$, we now give the dimensionally regularized expression for $R_t^{1+2} + R_c^{1+2} + R_c^3$.

$$\begin{aligned} R^{1+2} = & (K_{700} + K_{701}) \frac{\overline{m_W}^2}{i\epsilon} \ln r + g_1 \frac{\overline{m_W}^4}{2} + \frac{1}{2} K_{700} \ln^2 r \\ & + 2K_{700} \ln r \ln(m_b = m_W) - 2K_{700} \ln r + g_2 \ln(m_b = m_W) + g_3; \end{aligned} \quad (3.5)$$

The first term in eq. (3.5) is due to infrared singularities in the on-shell $b \rightarrow s$ amplitude as suggested by the notation $\frac{1}{i\epsilon}$. This term is entirely due to those diagrams in set 3 of Fig. 2 where the photon is radiated from the internal quark or the W (or γ) boson. The quantities g_1, g_2 and g_3 in eq. (3.5) can be written as ($z = (m_t = m_W)^2$, $\text{Li}(x) = \int_0^x \frac{dt}{t} \ln(1-t)$)

$$g_1 = \frac{(324z^4 - 450z^3 + 270z^2 + 72z) \ln z + 112z^5 + 244z^4 + 55z^3 - 931z^2 + 593z - 73}{72(z-1)^5} - \frac{35}{216} \quad (3.6)$$

⁶The reader who wishes to see the explicit form for \hat{R}_2 is referred to eq. (2.35) in ref. [13].

⁷We could separate ultraviolet and infrared poles in our calculation. In the following, $1 = i\epsilon$ ($1 = \epsilon$) stands for infrared (ultraviolet) poles.

$$g_2 = \frac{(216z^3 + 162z^2 - 72z) \ln z + 44z^4 + 154z^3 - 393z^2 + 274z - 79}{36(z-1)^4} - \frac{7}{4} \quad (3.7)$$

$$\begin{aligned} g_3 = & \frac{z(8z^3 + 61z^2 - 40z + 4)}{6(z-1)^4} \text{Li}(1 - \frac{1}{z}) + \frac{2}{3} i K_{800} + \frac{2}{27} z^2 + \frac{3155}{1296} \\ & (4860z^4 - 18954z^3 + 11502z^2 + 648z) \ln^2 z \\ & + (3240z^5 + 16956z^4 + 37638z^3 - 56586z^2 + 20688z - 2496 - 216 z^2 (z^3 - z^2)) \ln z \\ & + (1442z^5 - 55910z^4 + 109651z^3 - 69271z^2 + 20999z - 4027) \\ & + (60z^5 - 228z^4 + 636z^3 - 924z^2 + 552z - 96) z^2 = (1296(z-1)^5) \end{aligned} \quad (3.8)$$

3.2 Counterterms

The counterterms relevant for calculating on-shell matrix elements are generated by expressing the bare parameters in the original Lagrangian in terms of the renormalized quantities. Working up to order ϵ_s , the only parameters which need renormalization in the present situation are the t -quark mass and the b -quark mass (in principle also the s -quark mass if we did not work in the limit $m_s = 0$). Using on-shell renormalization for the external b -quark mass and \overline{MS} renormalization for the (internal) top quark mass, the connection between the bare and renormalized masses reads

$$\begin{aligned} m_{t,\text{bare}} &= m_t + \delta m_t ; \quad \frac{m_t}{m_t} = \frac{s}{4} C_F - \frac{3}{4} \\ m_{b,\text{bare}} &= m_b + \delta m_b ; \quad \frac{m_b}{m_b} = \frac{s}{4} C_F - \frac{3}{4} + 6 \ln(-m_b) + 4 \end{aligned} \quad (3.9)$$

Note, these mass shifts not only shift the mass terms like $m_t \bar{t}t$, but also the Yukawa terms like $g_b(m_b L - m_t R) \bar{t}$, where ϕ is the unphysical charged Higgs field which appears in covariant gauges. These counterterms, induced by the shifts δm_t and δm_b , generate corrections for the $b \rightarrow s$ matrix element, which we denote by M_b and M_t , respectively. Writing $M_f = V R_f$ ($f = t, b$) with V given in eq. (3.2), we get

$$\begin{aligned} R_b = & (6z - 8) \ln z - 7z^2 + 16z - 9 - \frac{2}{z} + 4 \ln(-m_b) + 8 = 3 \\ & + (6z + 8) \ln^2 z + (20z^2 - 26z) \ln z - 19z^2 + 44z - 25 - \frac{1}{m_W^2} \frac{z}{16(z-1)^3} \end{aligned} \quad (3.10)$$

while R_t is given by

$$\begin{aligned} R_t = & \frac{6}{z} (18z^3 + 30z^2 - 24z) \ln z - 47z^3 + 63z^2 - 9z - 7 + 18z (3z^2 - 5z + 4) \ln^2 z \\ & + (246z^3 + 114z^2 - 288z + 96) \ln z + 44z^4 - 547z^3 + 855z^2 - 413z + 61 - \frac{1}{m_W^2} \frac{z}{24(z-1)^5} \end{aligned} \quad (3.11)$$

When writing down the expression for R_b , we should mention, that we did not include the insertion of $m_b b b$ in the external b -quark leg. This is quite in analogy of omitting self-energy diagrams for the external legs. Such corrections on the external legs are taken into account by multiplying the amputated diagram with the factor $Z_{2;b} Z_{2;s}$, where $Z_{2;b}$ and $Z_{2;s}$ are the residues taken at the (physical) pole position of the regularized b - and s -quark two point functions, respectively. Making use of the expression (in Feynman gauge)

$$Z_2(m) = 1 - \frac{s}{4} C_F \frac{1}{m^2} \left(\frac{1}{\epsilon} + \frac{2}{\epsilon_{\text{ir}}} + 4 \right); \quad (3.12)$$

the counterterm M_{Z_2} induced by the Z_2 -factors of the external quark fields reads (again writing $M_{Z_2} = V R_{Z_2}$)

$$R_{Z_2} = \frac{1}{m_W^2} \left(\frac{2}{\epsilon_{\text{ir}}} (K_{700} + K_{701}) + \frac{1}{\epsilon} (K_{700} + K_{701}) \right) + \frac{3}{4} \ln(m_b/m_W) - \frac{3}{2} \ln r - K_{700}; \quad (3.13)$$

4 $b \rightarrow s$ in the effective theory

As in the full theory, we first discuss the matrix elements for $b \rightarrow s$ of the operators in basis (1.2). In section 4.2 we list the various counterterm contributions.

4.1 Regularized Feynman diagrams

We write the matrix element \hat{M}^i for $b \rightarrow s$ as a sum of the contributions due to the operators O_i in the effective Hamiltonian, i.e.,

$$\hat{M} = \sum_{i=1}^{X^8} \hat{M}^i; \quad \hat{M}^i = \frac{4iG_F t}{2} C_i \langle s | \mathcal{O}_i | b \rangle; \quad (4.1)$$

To facilitate later the comparison between the results in the two versions of the theory (full vs. effective), we write $\hat{M}^i = \hat{M}_0^i + \frac{s}{4} \hat{M}_1^i$ and cast the term proportional to $\frac{s}{4}$ in the form

$$\frac{s}{4} \hat{M}_1^i = V \hat{R}_i; \quad (4.2)$$

where V is given in eq. (3.2).

We first discuss the contributions of the four-Fermi operators $O_1 \dots O_6$. As the Wilson coefficients of O_1, O_3, O_4, O_5 and O_6 start at order $\frac{1}{s}$, we only have to take into account their order $\frac{0}{s}$ (one-loop) matrix elements; it is well-known that in the NDR scheme only O_5 and O_6 have a non-vanishing one-loop matrix element for $b \rightarrow s$. Making use of the Wilson coefficients (see [17])

$$C_5(\mu) = \frac{s(\mu)}{4} C_F \left(\frac{1}{6} \ln \frac{\mu}{m_W} - \frac{1}{8} \right); \quad C_6(\mu) = \frac{s(\mu)}{4} C_F \left(\frac{1}{2} \ln \frac{\mu}{m_W} + \frac{3}{8} \right); \quad (4.3)$$

\hat{R}_5 and \hat{R}_6 are readily obtained

$$\hat{R}_5 = \frac{1}{3} - \frac{1}{6} \ln \frac{z}{m_W} - \frac{1}{8} E' \quad ; \quad \hat{R}_6 = \frac{1}{2} \ln \frac{z}{m_W} + \frac{3}{8} E' \quad ; \quad (4.4)$$

with

$$E' = \frac{2}{3} \ln z + \frac{z^2 (15 - 16z + 4z^2)}{6(1-z)^4} \ln z + \frac{z(18 - 11z - z^2)}{12(1-z)^3} - \frac{2}{3} \quad : \quad (4.5)$$

On the other hand, the Wilson coefficient of the operator O_2 starts at order $\frac{0}{s}$. Consequently, we have to take in principle one- and two-loop matrix elements of this operator. In practice, however, the order $\frac{0}{s}$ (one-loop) matrix element of O_2 vanishes and therefore only the contribution of the order $\frac{1}{s}$ (two-loop) matrix element remains:

$$\hat{R}_2 = \quad : \quad (4.6)$$

As this contribution also occurs in the full theory result in section 3.1 (see eqs. (3.1) and (3.3)), the explicit expression for the r.h.s. of eq. (4.6) is not needed for the extraction of C_{71} .

The order $\frac{1}{s}$ contribution of the matrix elements of the dipole operator O_7 (see Figs. 4a,b) yields

$$\hat{R}_7 = \frac{3}{4} C_{71} - C_{70} \frac{\overline{m_W}^2}{i\epsilon} \ln r + \frac{C_{70}}{2} \ln^2 r + 2C_{70} \ln r \ln(m_b = m_W) - 2C_{70} \ln r \quad : \quad (4.7)$$

The first term on the r.h.s. of eq. (4.7) comes from the tree-level matrix element in Fig 4a, being multiplied with the the order $\frac{1}{s}$ part (i.e. C_{71}) of the Wilson coefficient C_7 . The remaining terms are due to the one-loop graph in Fig. 4b. Note that C_{71} is the quantity we ultimately wish to extract. Finally, the diagrams of O_8 are depicted in Figs. 4c,d; its contribution is [13]

$$\hat{R}_8 = \frac{C_{80}}{9} - \frac{12}{9} (33 + 2 \frac{1}{s} + 24 \ln(m_b = m_W) - 6i) \quad : \quad (4.8)$$

4.2 Counterterms

As the operators mix under renormalization, we have to consider counterterm contributions induced by operators of the form $C_i Z_{ij} O_j$. We denote their contributions to $b \rightarrow s$ by

$$\hat{M}_{ij} = \frac{4iG_F}{2} \text{tr} \left[\bar{\psi}_i Z_{ij} O_j \right] \quad : \quad (4.9)$$

The non-vanishing matrix elements read (using $\hat{M}_{ij} = V \hat{R}_{ij}$)

$$\hat{R}_{25} = \frac{1}{36} \frac{1}{m_b^2} \quad ; \quad \hat{R}_{26} = \frac{1}{4} \frac{1}{m_b^2} \quad ; \quad \hat{R}_{27} = \frac{29}{27} \frac{1}{s} \quad ; \quad \hat{R}_{77} = -\frac{4}{3} C_{70} \quad ; \quad \hat{R}_{87} = \frac{4}{3} C_{80} \quad ; \quad (4.10)$$

where we made use of the renormalization constants [4]

$$(Z_{25}; Z_{26}; Z_{27}; Z_{77}; Z_{87}) = \frac{s}{4} C_F \left(\frac{1}{12}; \frac{1}{4}; \frac{29}{27}; -\frac{4}{3}; \frac{4}{3} \right) \quad : \quad (4.11)$$

It is well-known that the renormalization of the four-Fermi operators requires the introduction of counterterms proportional to evanescent operators [26]. Calculating $b!$ s up to order s , there are potential counterterm contributions involving evanescent operators needed to renormalize O_2 . As the initial conditions for the four-Fermi operators (which we partially used in section 4.1) depend on the actual choice of the evanescent operators, we have to use the same set when calculating their effect of $b!$ s. We consistently take both, the initial conditions of the four-Fermi operators and the set of evanescent operators from refs. [17, 26, 27, 28]. The only potentially relevant matrix element of evanescent operators contributing $b!$ s is

$$\langle s | \frac{1}{2} E_1 [O_2] | b \rangle ; \quad (4.12)$$

where the evanescent operator $E_1 [O_2]$ is of the form

$$\begin{aligned} E_1 [O_2] &= [s_1 \quad L c_2 c_3 \quad L b_4 \quad (4 + a_1) s_1 \quad L c_2 c_3 \quad L b_4] K_{1234} \\ K_{1234} &= \frac{1}{2} \quad \frac{1}{6} : \end{aligned} \quad (4.13)$$

However, as these matrix elements are identically zero (in dimensions), there are no contributions from counterterms proportional to evanescent operators.

Besides the counterterms induced by operator mixing, we also have to renormalize the b -quark mass which explicitly appears in the operator O_7 and in addition we have to multiply the lowest order matrix element by the factor $Z_2(m_b) Z_2(m_s)$, quite in analogy to the calculation in the full theory. The counterterm due to the b -quark mass renormalization $\hat{M}_b = V \hat{R}_b$ yields

$$\hat{R}_b = \frac{3}{-} + 6 \ln(-m_b) + 4 C_{70} ; \quad (4.14)$$

when using the on-shell definition for the b -quark mass, while the counterterm $\hat{M}_{Z_2} = V \hat{R}_{Z_2}$ is given by

$$\hat{R}_{Z_2} = \frac{2}{m_W} \quad \frac{2}{ir} C_{70} + \frac{1}{-} C_{70} + 4 \quad 6 \ln(m_b = m_W) \quad \frac{3}{2} \ln r \quad C_{70} : \quad (4.15)$$

5 Extraction of $C_{71}(w_t)$

To summarize section 3, the order s part M_1^{ren} of the renormalized matrix element for $b!$ s in the full theory reads

$$\frac{s}{4} M_1^{\text{ren}} = V \left[R^{1+2} + \hat{R}_2 + R_b + R_t + R_{Z_2}^i \right] ; \quad (5.1)$$

where the quantities in the bracket on the r.h.s. of eq. (5.1) are given in eqs. (3.5), (3.3), (3.10), (3.11) and (3.13), respectively; the prefactor V is given in eq. (3.2).

The corresponding renormalized matrix element \hat{M}_1^{ren} in the effective theory can be obtained from the information in section 4; \hat{M}_1^{ren} reads

$$\frac{s}{4} \hat{M}_1^{\text{ren}} = V \left[\hat{R}_2 + \hat{R}_5 + \hat{R}_6 + \hat{R}_7 + \hat{R}_8 + \hat{R}_{25} + \hat{R}_{26} + \hat{R}_{27} + \hat{R}_{77} + \hat{R}_{87} + \hat{R}_b + \hat{R}_{Z_2}^i \right] ; \quad (5.2)$$

where the various quantities in the bracket are given in eqs. (4.6), (4.4), (4.7), (4.8), (4.10), (4.14) and (4.15).

Before we are able to correctly extract C_{71} , a remark concerning the infrared structure is in order. We split M_1^{ren} into an infrared singular and an infrared finite piece, i.e.,

$$M_1^{\text{ren}} = M_{1;\text{ir}}^{\text{ren}} + M_{1;\text{fin}}^{\text{ren}} ; \quad (5.3)$$

As this splitting is not unique (concerning the finite terms), we define the singular part to be

$$M_{1;\text{ir}}^{\text{ren}} = (K_{700} + K_{701}) \frac{\overline{m_W}^2}{\text{ir}} \ln r - 2 (K_{700} + K_{701}) \frac{\overline{m_W}^2}{\text{ir}} ; \quad (5.4)$$

where the first and second term on the r.h.s. are due to the two-loop diagrams (3.5) and the counterterms (3.13), respectively. We do now an analogous splitting for the renormalized matrix element in the effective theory, i.e.,

$$\hat{M}_1^{\text{ren}} = \hat{M}_{1;\text{ir}}^{\text{ren}} + \hat{M}_{1;\text{fin}}^{\text{ren}} ; \quad (5.5)$$

with

$$\hat{M}_{1;\text{ir}}^{\text{ren}} = C_{70} \frac{\overline{m_W}^2}{\text{ir}} \ln r - 2 C_{70} \frac{\overline{m_W}^2}{\text{ir}} ; \quad (5.6)$$

As the matching has to be done in four dimensions, we cannot – strictly speaking – use the process $b \rightarrow s$ to do the matching, because of the infrared singularities. To cancel these singularities, we have to include the gluon Bremsstrahlung process $b \rightarrow s g$ in both versions of the theory. In the effective theory, the process has been worked out in [6, 10, 12] (but the explicit result is not important here); the result in the full theory is obtained from the effective theory result by replacing C_{70} by $K_{700} + K_{701}$. The correct physical matching condition consists in requiring the infrared finite quantity $= (b \rightarrow s) + (b \rightarrow s g; E \rightarrow E^{\text{min}})$ to be equal in both versions of the theory. Due to the specific form of eqs. (5.3) { (5.6) and due to the specific difference in the bremsstrahlung contribution, it follows that the physical matching condition implies

$$M_{1;\text{fin}}^{\text{ren}} = \hat{M}_{1;\text{fin}}^{\text{ren}} ; \quad (5.7)$$

The extraction of C_{71} is now straightforward. In summary: Writing the Wilson coefficient $C_7(\mu_t)$ at the matching scale μ_t in the form

$$C_7(\mu_t) = C_{70}(\mu_t) + \frac{s}{4} C_{71}(\mu_t) ; \quad (5.8)$$

we obtain (in the naive dimensional regularization scheme)

$$\begin{aligned} C_{71}(\mu_t) = & \frac{2z(8z^3 + 61z^2 - 40z + 4)}{9(z-1)^4} \text{Li}\left(1 - \frac{1}{z}\right) + \frac{2z^2(3z^2 + 23z - 14)}{3(z-1)^5} \ln^2 z \\ & + \frac{2(51z^5 + 294z^4 + 1158z^3 - 1697z^2 + 742z - 116)}{81(z-1)^5} \ln z \\ & + \frac{1520z^4 + 12961z^3 - 12126z^2 + 3409z - 580}{486(z-1)^4} \\ & + \frac{4z^2(3z^2 + 23z - 14)}{3(z-1)^5} \ln z \ln(\mu_t = m_W) \\ & + \frac{2(106z^4 + 287z^3 + 1230z^2 - 1207z + 232)}{81(z-1)^4} \ln(\mu_t = m_W) ; \end{aligned} \quad (5.9)$$

Here, $z = (m_t(\mu_t) - m_W)^2$, where $m_t(\mu_t)$ is the \overline{MS} top quark mass at the renormalization scale μ_t . The lowest order function C_{70} is given in eq. (2.24).

Taking into account that the result of Adel and Yao [1] is given in the so-called R renormalization scheme, we got the same result for $C_{71}(\mu_t)$.

6 $b \rightarrow s$ in the full theory

As in the $b \rightarrow s$ case we first give the results for the two-loop diagrams and then move to the counterterm contributions.

6.1 Two-loop Feynman diagrams

We again write the $b \rightarrow s$ matrix element M in the form $M = M_0 + \frac{s}{4} M_1$. Using the "reduction technique" described in section 2.3, the complete set of two-loop Feynman graphs is given by the abelian diagrams in Fig. 2 and by the non-abelian diagrams in Fig. 3, which involve the triple gluon coupling. The crosses in Fig. 2 and Fig. 3 show the possible locations from where the gluon can be emitted. Of course the graphs with a cross at the W line in Fig. 2 have to be omitted. Working in the limit $m_s = 0$, diagram 5b in Fig. 2 vanishes. It is convenient to write M_1 in the form

$$\frac{s}{4} M_1 = W \left[Q_t^{1+2} + Q_c^{1+2} + Q_c^3 \right]; \quad (6.1)$$

where the quantity W is defined as

$$W = \frac{4ig_F}{p^2} \frac{t}{2} \frac{s}{4} \text{hsg} \mathcal{D}_8 \mathcal{P}_{\text{tree}}; \quad (6.2)$$

In eq. (6.1) Q_f^{1+2} denotes the sum of the first and second contribution in the Heavy Mass Expansion for an internal quark of flavor f ($f = t, c$); Q_c^3 is the third contribution in this expansion, which only has to be considered for the light internal quarks. Like R_c^3 in eq. (3.1) of section 3.1, Q_c^3 is just

$$Q_c^3 = \hat{Q}_2; \quad (6.3)$$

where \hat{Q}_2 is the quantity defined through the relation

$$\text{hsg} \mathcal{D}_2 \mathcal{P}_i = \frac{s}{4} \text{hsg} \mathcal{D}_8 \mathcal{P}_{\text{tree}} \hat{Q}_2; \quad (6.4)$$

As exactly the same term also appears in the effective theory, Q_c^3 drops out when extracting the $O(s)$ correction to the Wilson coefficient C_8 .

The dimensionally regularized expressions for Q_t^{1+2} , Q_c^{1+2} , Q_c^{1+2} can be written in the form

$$Q^{1+2} = \frac{1}{6} (K_{800} + K_{801}) \frac{\overline{m_W}^2}{\text{ir}} \ln r - 3 (K_{800} + K_{801} + {}^2 K_{802}) \frac{\overline{m_W}^2}{\text{ir}^2} \\ - \frac{3}{2} (K_{800} + K_{801}) \frac{\overline{m_W}^2}{\text{ir}} [2 + \ln r - 4 \ln(m_b - m_W) + 2i\pi]$$

$$\begin{aligned}
& + h_1 \frac{1}{m_W^4} + h_2 \ln^2 r + h_3 \ln r \ln(m_b = m_W) + h_4 \ln r \\
& + h_5 \ln(m_b = m_W) + h_6 \ln^2(m_b = m_W) + h_7 :
\end{aligned} \tag{6.5}$$

The first term on the r.h.s. of eq. (6.5) is due to infrared singularities coming from the (abelian) graph in set 3 in Fig. 2, where the gluon is radiated from the internal quark; the infrared structures appearing in the second and third term are due to non-abelian diagrams in Fig. 3. Eq. (6.5) shows that the infrared singularities again just multiply the dimensionally regularized version of the lowest order matrix element (see eqs. (2.20) and (2.21)).

The functions K_{800} and K_{801} appearing in eq. (6.5) are given in eqs. (2.25) and (2.27). We note that the function K_{802} is not needed explicitly in order to extract C_{81} , as we will see later. The functions h_i in eq. (6.5) read ($z = (m_t = m_W)^2$)

$$h_1 = \frac{z(774z^2 + 810z + 144) \ln z + 137z^5}{72(z-1)^5} - \frac{823z^4 + 257z^3}{425z^2 + 958z} - \frac{104}{27} \tag{6.6}$$

$$h_2 = \frac{2}{3} K_{800} ; h_3 = \frac{8}{3} C K_{800} ; h_4 = \frac{8}{3} K_{800} ; h_6 = 6 K_{800} \tag{6.7}$$

$$h_5 = \frac{z(162z - 72) \ln z + 11z^4}{18(z-1)^4} - \frac{110z^3 + 57z^2 + 82z}{40} + 6i K_{800} \tag{6.8}$$

$$\begin{aligned}
h_7 = & \frac{z(4z^3 - 40z^2 - 41z - 1) \text{Li}(1 - \frac{1}{z})}{6(z-1)^4} - \frac{8}{3} i K_{800} - \frac{59}{108} - \frac{185}{324} \\
& (35964z^3 + 54756z^2 + 2592z) \ln^2 z \\
& + 7452z^5 - 42660z^4 - 92772z^3 - 73164z^2 + 48984z - 3360 + 3186(z^3 - z^2) \ln z \\
& + (844z^5 + 40012z^4 + 90580z^3 - 148588z^2 + 16688z + 464) \\
& + (885z^5 + 3363z^4 - 9381z^3 + 13629z^2 - 8142z + 1416) = (2592(z-1)^5)
\end{aligned} \tag{6.9}$$

6.2 Counterterms

As the discussion concerning the counterterms induced by the shifts in the t - and b -quark masses is exactly the same as in the $b \rightarrow s$ process in section 3.2, we give immediately the result. Writing $M_f = W Q_b$ ($f = t, b$) with W given in eq. (6.2), we get

$$\begin{aligned}
Q_b = & 2 \ln z + z^2 - 4z + 3 - \frac{2}{m_W^2} + 4 \ln(-m_b) + 8 = 3 \\
& + 2 \ln^2 z + 2z(z-4) \ln z - z^2 + 8z - \frac{7}{m_W^2} - \frac{z}{2(z-1)^3}
\end{aligned} \tag{6.10}$$

$$Q_t = \frac{6}{m_W^2} \left[6z(z+1) \ln z + z^3 + 9z^2 - 9z - 1 + 18z(z+1) \ln^2 z \right. \\ \left. + (6z^3 - 84z^2 - 18z + 24) \ln z + 5z^4 - 10z^3 + 126z^2 - 158z + 37 \right] \\ - \frac{z}{3(z-1)^5} \quad (6.11)$$

Also the counterterms due to the $\frac{P}{Z_2}$ factors of the external quark fields are obtained in the same manner as in section 3.2, leading to $(M_{Z_2} = W - Q_{Z_2})$

$$Q_{Z_2} = \frac{1}{m_W^2} \left[\frac{4}{3} \frac{2}{ir} (K_{800} + K_{801}) + \frac{1}{2} (K_{800} + K_{801}) \right. \\ \left. + 4 - 6 \ln(m_b/m_W) - \frac{3}{2} \ln r - K_{800} \right] : \quad (6.12)$$

For the $b \rightarrow sg$ case there are additional counterterm contributions due to the strong coupling constant renormalization and due to the $\frac{P}{Z_3}$ factor associated with the external gluon. Denoting the combined effect by $M_g = W - Q_g$, one obtains

$$Q_g = \frac{3}{2} + f - (K_{800} + K_{801}) : \quad (6.13)$$

As the finite term f will appear also in the corresponding counterterm in the effective theory, it will drop out when extracting C_{81} .

7 $b \rightarrow sg$ in the effective theory

7.1 Regularized Feynman diagrams

In the effective theory the matrix element \hat{M} for $b \rightarrow sg$ is of the form

$$\hat{M} = \sum_{i=1}^{X^8} \hat{M}^i ; \quad \hat{M}^i = \frac{4iG_F}{2} C_i \text{hs}g \bar{D}_i \text{bi} : \quad (7.1)$$

We write $\hat{M}^i = \hat{M}_0^i + \frac{s}{4} \hat{M}_1^i$ and put the term proportional to s into the form

$$\frac{s}{4} \hat{M}_1^i = W \hat{Q}_i ; \quad (7.2)$$

where W is given in eq. (6.2). As the discussion how to get the quantities \hat{Q}_i is basically identical as in the $b \rightarrow s$ case in section 4.1, we just give the results. Among the four-Fermi operators, only O_2 and O_5 yield non-vanishing matrix elements for $b \rightarrow sg$. We get

$$\hat{Q}_2 ; \quad \hat{Q}_5 = \frac{2}{9} \ln \frac{2}{m_W} - \frac{1}{6} E ; \quad (7.3)$$

where E is given in eq. (4.5). Again, we do not have to know \hat{Q}_2 explicitly, because this term also appears in the full theory result; it drops out when extracting C_{81} .

While there is no contribution from the dipole operator O_7 , there are various diagrams associated with the operator O_8 (see Figs. 5,6). The sum of all these contributions is given by

$$\begin{aligned}\hat{Q}_8 = & \frac{1}{6} C_{80} \frac{\overline{m_W}^2}{\epsilon_{\text{ir}}} \ln r - 3 C_{80} \frac{\overline{m_W}^2}{\epsilon_{\text{ir}}} \left[2 + \ln r - 4 \ln(m_b = m_W) + 2i \right] \\ & + C_{80} \frac{11}{3} \frac{\overline{m_W}^2}{\epsilon_{\text{ir}}} + 6i \ln(m_b = m_W) - \frac{8}{3}i + \frac{2}{3} \ln^2 r - 6 \ln^2(m_b = m_W) \\ & \frac{8}{3} \ln r + \frac{8}{3} \ln r \ln(m_b = m_W) - \frac{4}{3} \ln(m_b = m_W) + \frac{1}{3} + \frac{59}{36} \epsilon_{\text{ir}}^2 + C_{81} : \quad (7.4)\end{aligned}$$

When comparing with the full-theory expression \hat{Q}^{1+2} in eq. (6.5), one immediately realizes the correspondence of the infrared singularities. To this end it is important that one carefully disentangles everywhere infrared and ultraviolet poles. Especially, one should use the formula

$$\int \frac{d^d r}{(2\pi)^d} \frac{1}{(r^2)^2} = \frac{i}{16\pi^2} - \frac{1}{\epsilon_{\text{ir}}} \quad \text{instead of} \quad \int \frac{d^d r}{(2\pi)^d} \frac{1}{(r^2)^2} = 0 : \quad (7.5)$$

An example, where such a situation occurs, is the diagram in Fig 6c.

7.2 Counterterms

As the operators mix under renormalization we have to consider counterterm contributions induced by operators of the form $C_i Z_{ij} O_j$. We denote their contributions to $b \rightarrow s$ by

$$\hat{M}_{ij} = \frac{4iG_F}{2} t \text{sgn} C_i Z_{ij} O_j : \quad (7.6)$$

The non-vanishing matrix elements read (using $\hat{M}_{ij} = W \hat{Q}_{ij}$)

$$\hat{Q}_{25} = \frac{1}{9} \frac{1}{m_b} \epsilon_{\text{ir}}^2 ; \quad \hat{Q}_{28} = \frac{19}{27} \frac{1}{\epsilon_{\text{ir}}} ; \quad \hat{Q}_{88} = \frac{14}{3} \frac{1}{\epsilon_{\text{ir}}} C_{80} ; \quad (7.7)$$

where we made use of the renormalization constants [4]

$$Z_{25} = \frac{1}{9} \frac{s}{4} ; \quad Z_{28} = \frac{19}{27} \frac{s}{4} ; \quad Z_{88} = \frac{14}{3} \frac{s}{4} : \quad (7.8)$$

We note that there are no contributions to \hat{M} ($b \rightarrow s$) from counterterms proportional to evanescent operators.

In analogy to the $b \rightarrow s$ case in section 4.2, there are the counterterms from renormalizing the b -quark mass which explicitly appear in the definition of the operator O_8 and from the \overline{Z}_2 factors for the external quarks. The counterterm due to the b -quark mass renormalization $\hat{M}_b = W \hat{Q}_b$ yields

$$\hat{Q}_b = \frac{4}{3} \epsilon_{\text{ir}}^3 + 6 \ln(\epsilon_{\text{ir}} m_b) + 4 C_{80} ; \quad (7.9)$$

when using the on-shell definition for the b-quark mass (3.9), while the counterterm $\hat{M}_{Z_2} = W \hat{Q}_{Z_2}$ is given by

$$\hat{Q}_{Z_2} = \frac{1}{m_W^2} \left[\frac{4}{3} \frac{2}{\epsilon_{\text{ir}}} C_{80} + \frac{1}{4} C_{80} + 6 \ln(m_b/m_W) - \frac{3}{2} \ln r \right] C_{80} \quad ; \quad (7.10)$$

Finally, there are counterterms due to the strong coupling constant renormalization and due to the Z_3 of the external gluon. As in the full theory, we only give the combined counterterm $\hat{M}_g = W \hat{Q}_g$

$$\hat{Q}_g = \frac{3}{4} + f C_{80} \quad ; \quad (7.11)$$

As f is the same finite quantity as in the corresponding result (6.13) obtained in the full theory, we do not need its explicit form, because it drops out when extracting C_{81} .

8 Extraction of $C_{81}(w, t)$

To summarize section 6, the order s part M_1^{ren} of the renormalized matrix element for $b \rightarrow s g$ in the full theory is given by

$$\frac{s}{4} M_1^{\text{ren}} = W \left[Q^{1+2} + \hat{Q}_2 + Q_b + Q_t + Q_{Z_2} + Q_g \right] \quad ; \quad (8.1)$$

where the quantities in the bracket on the r.h.s. of eq. (8.1) are given in eqs. (6.5), (6.3), (6.10), (6.11), (6.12) and (6.13), respectively; the prefactor W is given in eq. (6.2).

The corresponding renormalized matrix element in the effective theory can be obtained from the information in section 7; \hat{M}_1^{ren} reads

$$\frac{s}{4} \hat{M}_1^{\text{ren}} = W \left[\hat{Q}_2 + \hat{Q}_5 + \hat{Q}_8 + \hat{Q}_{25} + \hat{Q}_{28} + \hat{Q}_{88} + \hat{Q}_b + \hat{Q}_{Z_2} + \hat{Q}_g \right] \quad ; \quad (8.2)$$

where the various quantities in the bracket are given in eqs. (7.3), (7.4), (7.7), (7.9), (7.10) and (7.11).

Before we extract C_{81} , which enters \hat{M}_1^{ren} via \hat{Q}_8 (see eq. (7.4)), we should point out that the discussion concerning the infrared singularities is similar as in the $b \rightarrow s$ case in section 5; all the formulae are written in such a way that we simply can discard the terms proportional to the poles in ϵ_{ir} in both versions of the theory. The extraction of C_{81} is then straightforward.

To summarize: Writing the Wilson coefficient $C_8(w, t)$ at the matching scale w, t in the form

$$C_8(w, t) = C_{80}(w, t) + \frac{s}{4} C_{81}(w, t) \quad ; \quad (8.3)$$

we obtain (in the naive dimensional regularization scheme)

$$\begin{aligned} C_{81}(w, t) = & \frac{z(4z^3 - 40z^2 + 41z - 1)}{6(z-1)^4} \text{Li}\left(1 - \frac{1}{z}\right) - \frac{z^2(17z + 31)}{2(z-1)^5} \ln^2 z \\ & - \frac{210z^5 - 1086z^4 + 4839z^3 - 3007z^2 + 2114z - 304}{216(z-1)^5} \ln z \\ & + \frac{611z^4 - 13346z^3 + 29595z^2 + 1510z - 652}{1296(z-1)^4} + \end{aligned}$$

$$+ \frac{z^2 (17z + 31)}{(z - 1)^5} \ln z \ln \frac{m_t}{m_W} + \frac{89z^4 - 446z^3 - 1437z^2 - 950z + 152}{54(z - 1)^4} \ln \frac{m_t}{m_W} : \quad (8.4)$$

Here, $z = (m_t(m_t) = m_W)^2$, where $m_t(m_t)$ is the \overline{MS} top quark mass at the renormalization scale m_t . The lowest order function C_{80} is given in eq. (2.25).

Taking into account that the result of Adel and Yao [1] is given in the so-called R renormalization scheme, our result is identical.

9 Summary

The order α_s corrections to the Wilson coefficients C_7 and C_8 are a very crucial ingredient for the prediction of the branching ratio for $b \rightarrow X_s \gamma$ in next-to-leading logarithmic precision. As these corrections, which involve many two-loop diagrams in the full theory, have been calculated so far by one group [1] only, we presented in this work a detailed recalculation. We extracted the $O(\alpha_s)$ corrections to C_7 and C_8 by comparing the on-shell processes $b \rightarrow s$ and $b \rightarrow sg$ in both versions of the theory. We evaluated the two-loop integrals in the full theory by using the Heavy Mass expansion method. Our α_s corrections (C_{71} and C_{81}) to the Wilson coefficients C_7 and C_8 completely agree with the findings of Adel and Yao.

We should point out that our result (as well as Adel and Yao's) for $C_{71}(m_t)$ and $C_{81}(m_t)$ is a priori specific to the basis given in eq. (1.2). However, the same answer is obtained for these Wilson coefficients when working in the basis recently used by Chetyrkin, Misiak and Munz.

Acknowledgments

We thank A. Ali, M. Misiak, U. Nierste and S.J. Rey for helpful discussions.

References

- [1] K. Adel and Y.-P. Yao, Phys. Rev. D 49 (1994) 4945.
- [2] A.F. Falk, M. Luke and M. Savage, Phys. Rev. D 49 (1994) 3367.
- [3] M.B. Voloshin, hep-ph/9612483.
Z. Ligeti, L. Randall and M.B. Wise, hep-ph/9702322.
A.K. Grant, A.G.Morgan, S. Nussinov and R. S. Pecci, hep-ph/9702380.
- [4] M. Ciuchini, E. Franco, G. Martinelli, L. Reina and L. Silvestrini, Phys. Lett. B 316 (1993) 127; Nucl. Phys. B 415 (1994) 403;
G. Cella, G. Curci, G. Ricciardi and A. Vicere, Phys. Lett. B 325 (1994) 227.
M. Misiak, Nucl. Phys. B 393 (1993) 23; Erratum ibid. B 439 (1995) 461.

- [5] M .S.A lam et al. (CLEO Collaboration), Phys.Rev.Lett. 74 (1995) 2885.
- [6] A .A li and C .G reub, Z .Phys. C 49 (1991) 431;
- [7] A .A li and C .G reub, Z .Phys. C 60 (1993) 433.
- [8] A .J.Buras, M .M isiak, M .M unz, and S .Pokorski, Nucl. Phys. B 424 (1994) 374.
- [9] M .C iuchini, E .Franco, G .M artinelli and L .Reina, Phys. Lett. B 334 (1994) 137.
- [10] A .A li and C .G reub, Phys. Lett. B 361 (1995) 146.
- [11] R .D .D ikem an, M .Shifm an and R .G .U raltsev, Int. J. M od. Phys. A 11 (1996) 571.
- [12] N .Pott, Phys. Rev. D 54 (1996) 938.
- [13] C .G reub, T .Hurth and D .W yler, Phys. Lett. B 380 (1996) 385; Phys. Rev. D 54 (1996) 3350.
- [14] K .Chetyrkin, M .M isiak and M .M unz, hep-ph/9612313.
- [15] B .G rinstein, R .Springer, and M .B .W ise, Phys. Lett. 202 (1988) 138; Nucl Phys. B 339 (1990) 269.
- [16] S .G .G orishny, preprints JINR E2-86-176, E2-86-177 (Dubna 1986); Nucl. Phys. B 319 (1989) 633.
S .G .G orishny and S .A .Larin Nucl. Phys. B 283 (1987) 452.
K .G .Chetyrkin, Teor. M at. F iz 75 (1988) 26; 76 (1988) 207. V A .
V A .Sm imov, Comm un. M ath. Phys. 134 (1990) 109; M od. Phys. Lett. A 10 (1995) 1485; hep-th/9608151.
- [17] A .J.Buras, M .Jam in, M .E .Lautenbacher and P .H .W eisz, Nucl. Phys. B 370 (1992) 69; Nucl. Phys. B 375 (1992) 501 (addendum).
- [18] M .C iuchini, E .Franco, G .M artinelli and L .Reina, Nucl. Phys. B 415 (1994) 403.
- [19] H .D .Politzer, Nucl. Phys. B 172 (1980) 349;
H .S im m a, Z .Phys. C 61 (1994) 67.
- [20] V A .Sm imov, Renorm alization and A sym ptotic Expansions, B irkhauser, Basel, 1991.
- [21] W .Z im m erm ann, Ann. Phys. 77 (1973) 570.
- [22] S .A .Anikin and O .I. Zaviabv, Teor. M at. F iz. 27 (1976) 425; Ann. Phys. 116 (1978) 135.
- [23] A .C .H eam, REDUCE User's M anual, The R and C oorporation, Santa M onica, Califomia, 1987.
- [24] A .Heck, Introduction to Maple, Springer-Verlag New York, Inc., (1993), ISBN 0-387-97662-0.
- [25] T .Inam i and C .S .L in , Prog. Theor. Phys. 65 (1981) 297.

- [26] A.J.Buras, P.H.Weisz Nucl.Phys.B 333 (1990) 66.
- [27] S.Herrlich and U.Nierste, Nucl.Phys.B 455 (1995) 39.
- [28] S.Herrlich and U.Nierste, Nucl.Phys.B 476 (1996) 27.

Figure Captions

Figure 1

- a Lowest order diagram for $b \rightarrow s \gamma$ in the full-theory. A cross denotes a possible location where the photon can be emitted. The wavy line stands for a W or unphysical Higgs boson (H). In the $b \rightarrow s \gamma$ case the cross at the $W = H$ has to be ignored.
- b Typical two-loop graph for $b \rightarrow s \gamma$.
- c-e Subdiagrams of b) which contribute in the Heavy Mass Expansion. See text.

Figure 2

Complete list of two-loop diagrams for $b \rightarrow s \gamma$ in the full-theory. A cross corresponds to a possible location for the photon emission. For the $b \rightarrow s \gamma$ process, this figure is a complete list of diagrams not involving the gluon triple coupling. (In the $b \rightarrow s \gamma$ case the crosses at the wavy ($W = H$) lines should be ignored.)

Figure 3

Complete list of two-loop diagrams involving the triple gluon vertex (for the $b \rightarrow s \gamma$ process).

Figure 4

Diagrams associated with the operators O_7 and O_8 in the effective theory for $b \rightarrow s \gamma$. See text.

Figure 5

Abelian diagrams associated with the operator O_8 in the effective theory for $b \rightarrow s \gamma$. See text.

Figure 6

Non-Abelian diagrams associated with the operator O_8 in the effective theory for $b \rightarrow s \gamma$. See text.

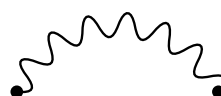
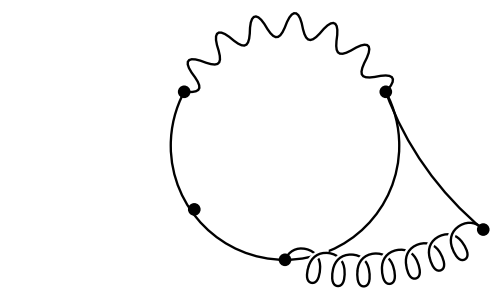
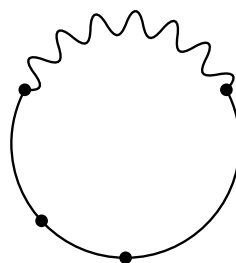
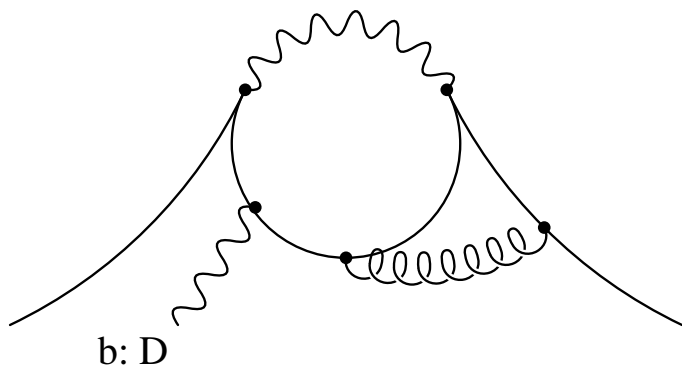
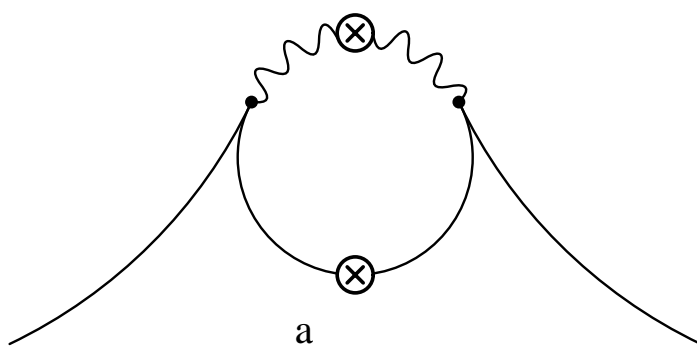


Figure 1

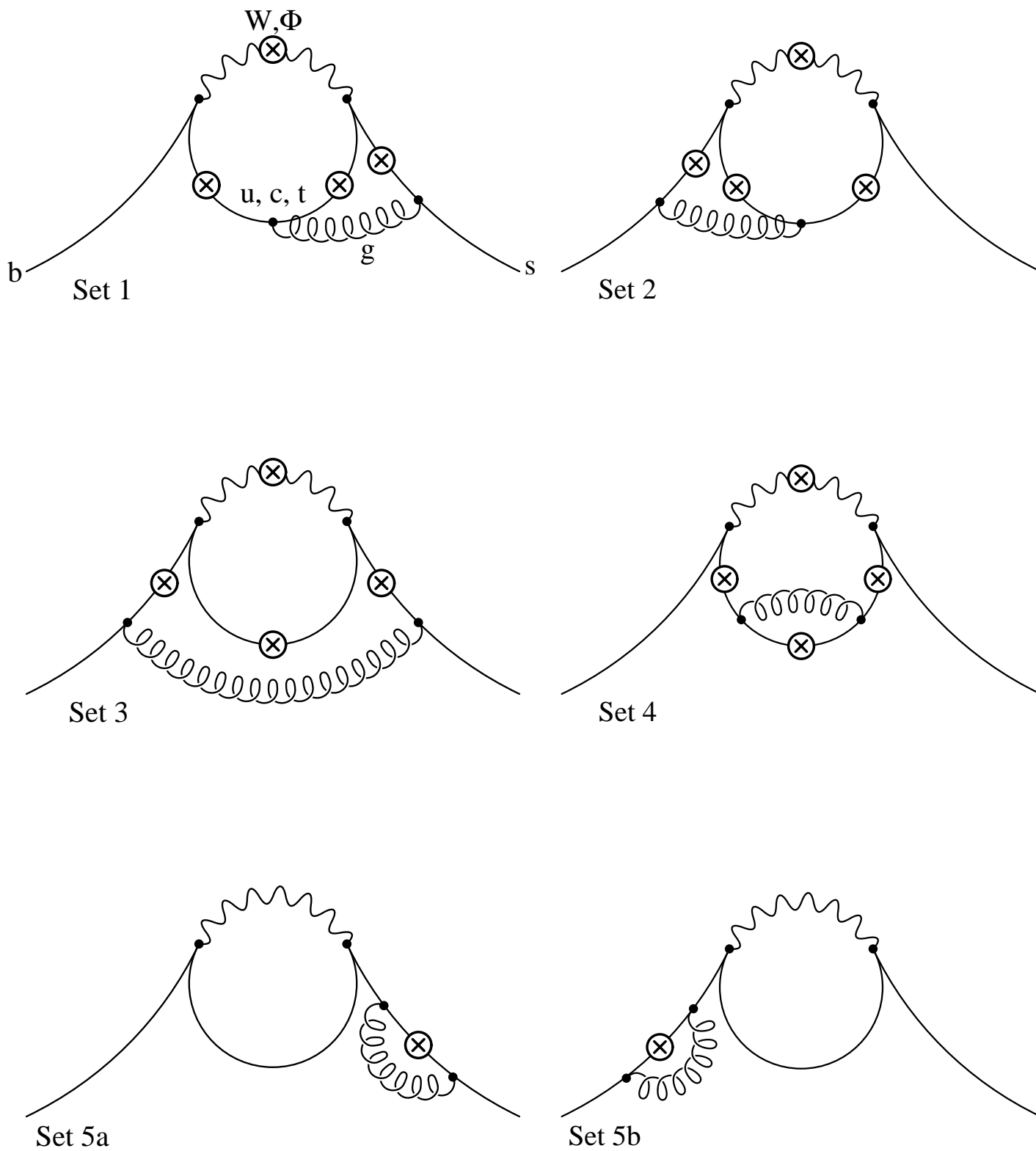


Figure 2

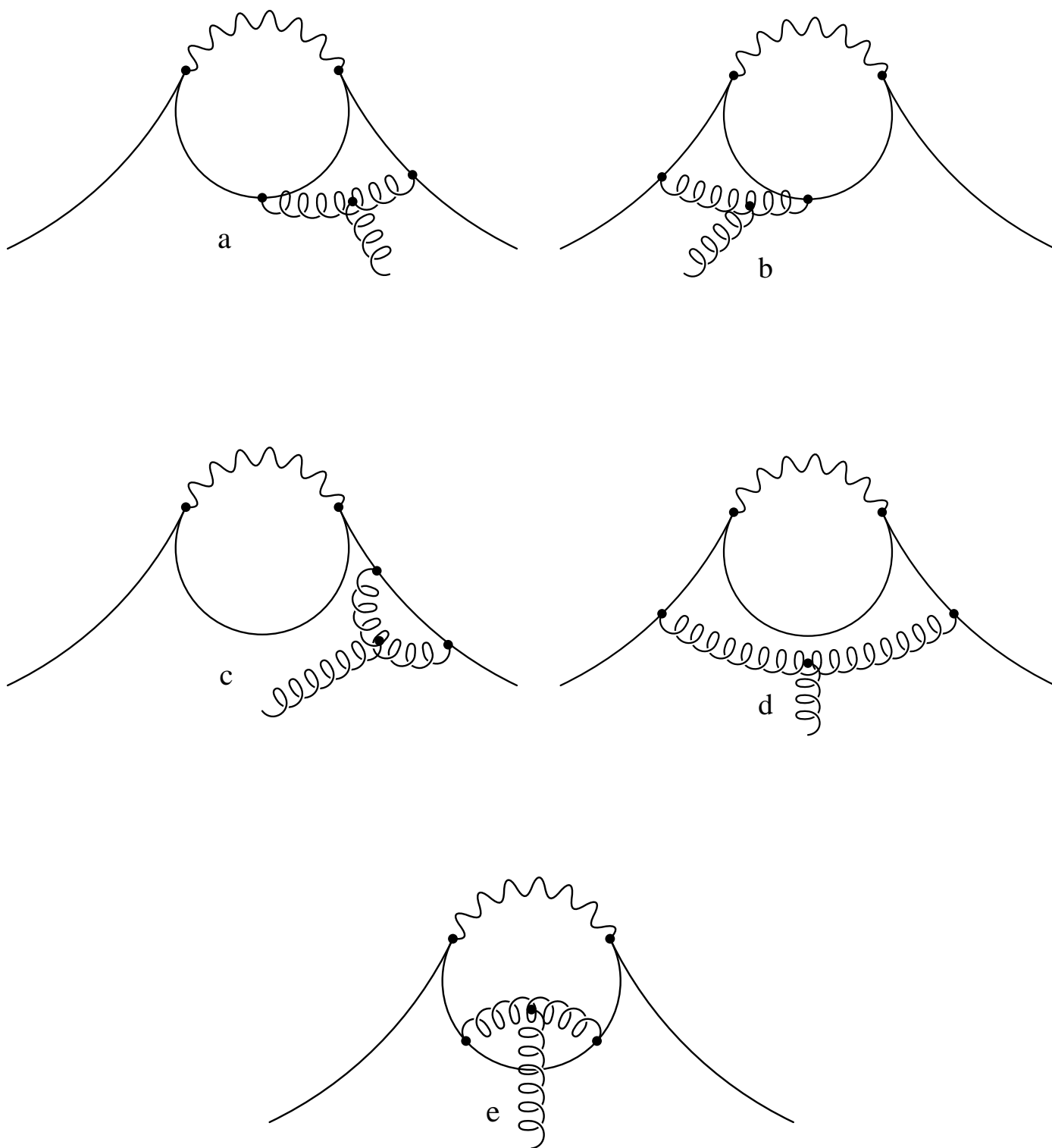


Figure 3

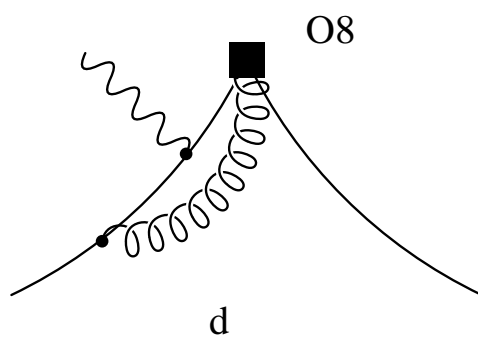
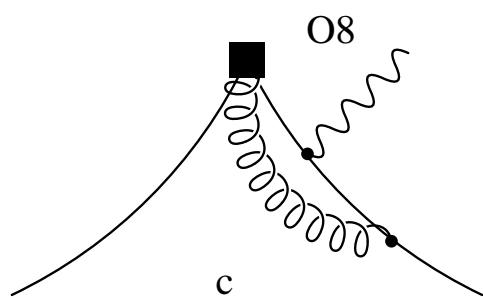
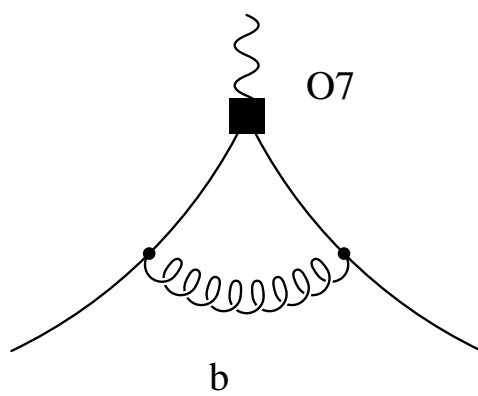
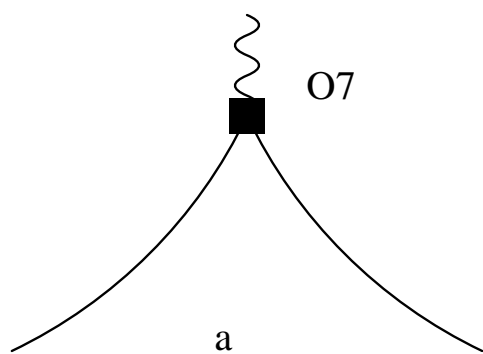


Figure 4

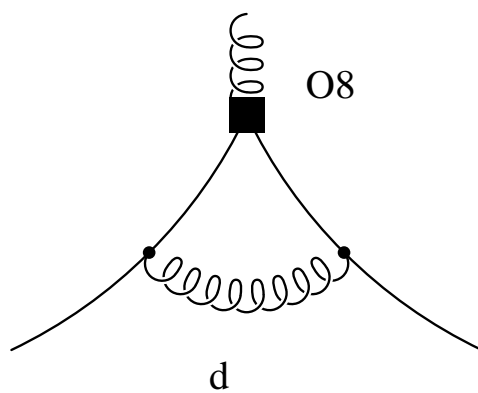
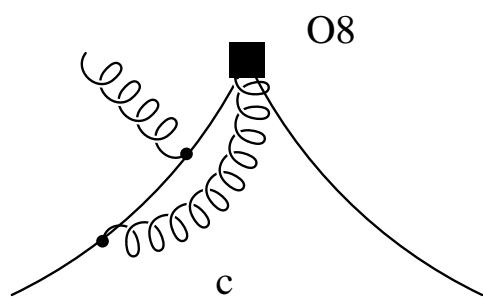
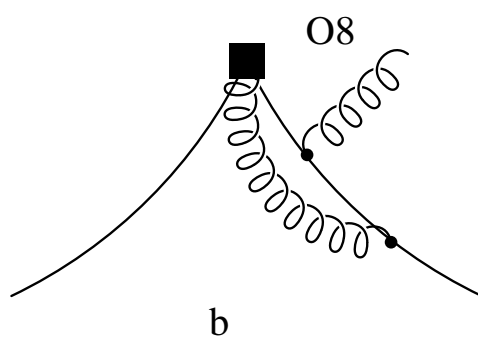
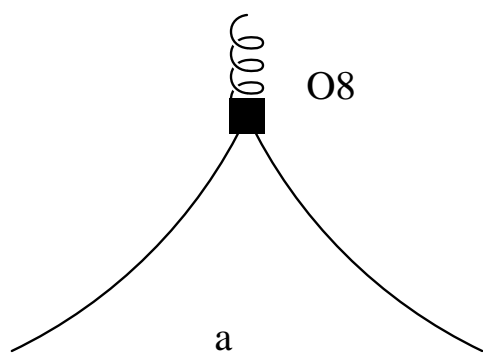


Figure 5

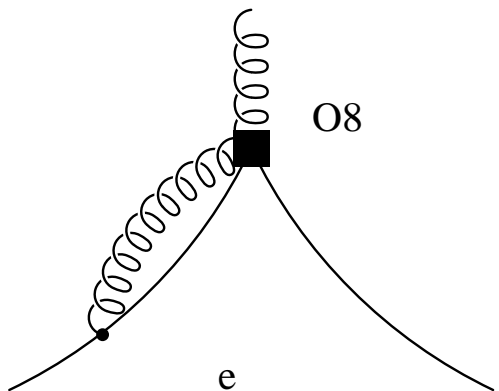
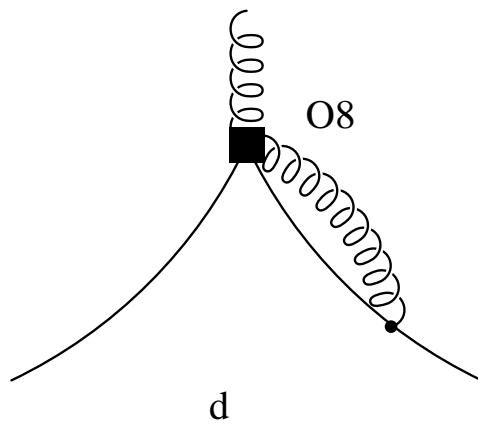
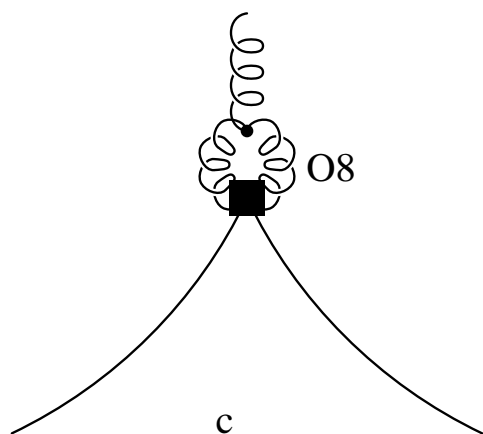
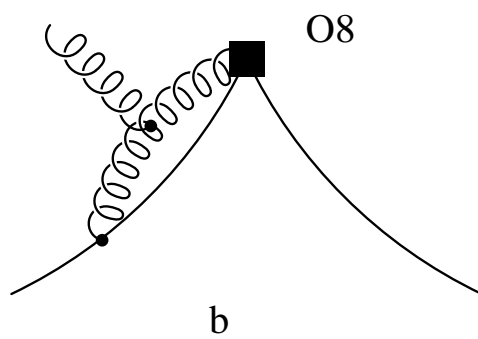
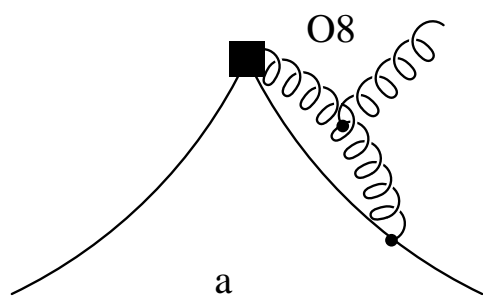


Figure 6